Reconfigurable Intelligent Surface-Aided Wireless Communication Considering Interference Suppression

Tong Van Luyen[1](✉), Le Van Thai[1], Nguyen Minh Tran[2], and Nguyen Van Cuong[1]

[1] Hanoi University of Industry, Hanoi, Vietnam
luyentv@haui.edu.vn

[2] Department of Electrical and Computer Engineering, Sungkyunkwan University, Suwon, South Korea

Abstract. As the demand for efficient wireless communication grows, radio frequency (RF) wireless communication emerges as a promising solution, facilitated by recent advancements in signal processing. A pivotal technology driving the efficacy of RF wireless communication is the reconfigurable intelligent surface (RIS). RIS enables passive beamforming and beam focusing, eliminating the need for power-hungry active components. In the era of the Internet of Things, electromagnetic environments are teeming with a multitude of devices, increasing the likelihood of interference. In response to this challenge, this paper presents a novel approach that leverages reconfigurable intelligent surfaces to focus power beams precisely on receivers while suppressing interference. Our research results demonstrate that this approach, based on least squares, outperforms nature-inspired optimization methods. The proposed technique not only enhances the efficiency of wireless communication but also ensures interference-free operation in complex electromagnetic environments. This study contributes to the growing body of knowledge in RF wireless communication and reconfigurable intelligent surfaces, offering a robust solution for the emerging IoT landscape.

Keywords: Reconfigurable intelligent surface · Wireless communication · Interference Suppression · Least squares

1 Introduction

The rapid advancement of wireless communication and power transfer technologies has brought forth a new era of connectivity and energy harvesting. In this context, Reconfigurable Intelligent Surfaces (RIS), also known as intelligent reflecting surfaces or metasurfaces, have emerged as a promising technology to revolutionize wireless communication and wireless communication systems. By actively controlling the electromagnetic (EM) waves in real-time, RIS offers the potential to enhance the efficiency and reliability of wireless communication systems while mitigating interference issues [1].

N. Thi Dieu Linh et al. (Eds.): ADHOCNETS 2023, LNICST 558, pp. 86–98, 2024.
https://doi.org/10.1007/978-3-031-55993-8_7

Besides, the field of wireless communication has witnessed substantial progress in recent years, with various technologies such as magnetic resonance coupling, inductive coupling, and microwave-based power transfer gaining prominence. These technologies have enabled wireless charging solutions for a range of applications, including smartphones, electric vehicles, and biomedical devices. However, challenges persist, particularly regarding the efficiency and distance limitations of these systems [2, 3].

In wireless communication, RIS has shown promise in enhancing signal quality, extending coverage, and reducing interference. In the context of wireless communication, RIS presents a novel opportunity to improve power transfer efficiency and mitigate interference. Meanwhile, interference from external sources and neighboring devices is a critical concern in wireless communication systems. These sources can significantly degrade power transfer efficiency and, in some cases, pose safety risks. Various methods have been proposed to address interference issues, including beamforming, interference cancellation techniques, and spatial modulation. However, integrating RIS into wireless communication systems for interference suppression represents a relatively unexplored area of research [4, 5].

This paper explores the integration of RIS into wireless communication systems and investigates the crucial aspect of interference suppression. The objective is to propose a reconfigurable intelligent surface-aided wireless communication approach that not only maximizes power transfer efficiency but also effectively suppresses interference from nearby sources. This approach encompasses four steps: (i) Estimate channels between the transmitter, receiver, and the RIS; (ii) Determine the directions of receivers; (iii) Find the optimal reflection coefficient vectors; and (iv) Conduct pattern nulling. By simulation, we have proven that the proposed approach can well form the power beam toward receivers while suppressing interference. Therefore, this research will hold significant implications for various applications, including IoT, electric vehicle charging, and remote powering, where efficient and interference-free wireless communication is essential.

The rest of the paper is organized as follows. Section 2 presents the system model. In the next Section, we thoroughly explain the four-step proposed approach. Section 4 shows the simulation results before concluding in Sect. 5.

2 System Model

We consider an RF wireless communication system with one transmitter, one receiver, and one RIS. The three-dimensional spatial model of the considered system is given in Fig. 1. The transmitter sends an EM power beam to the receiver with the assistance of the RIS. The RIS is a planar array with size of MN and is located at the origin of the system's global coordinate. The position of the unit cell (m, n) in the RIS is $\mathbf{q}_{m,n}^{\mathrm{RIS}} = \left(q_{m,n}^{\mathrm{RIS,x}}, q_{m,n}^{\mathrm{RIS,y}}, q_{m,n}^{\mathrm{RIS,z}}\right)^T$. The transmitter is position at $\mathbf{q}^{\mathrm{Tx}} = \left(q^{\mathrm{Tx,x}}, q^{\mathrm{Tx,y}}, q^{\mathrm{Tx,z}}\right)^T$, while the receiver is freely mobile with the location of $\mathbf{q}^{\mathrm{Rx}} = \left(q^{\mathrm{Rx,x}}, q^{\mathrm{Rx,y}}, q^{\mathrm{Rx,z}}\right)^T$. The transmitter sends an EM power beam to the receiver with the assistance of the RIS. The distance between the transmitter and the unit cell (m, n) in the RIS can be derived as [6].

$$d_{m,n}^{\mathrm{Tx-RIS}} = r^{\mathrm{Tx-RIS}} - \left(\boldsymbol{\delta}^{\mathrm{RIS-Tx}}\right)^T \mathbf{q}_{m,n}^{\mathrm{RIS}}, \tag{1}$$

where $r^{\text{Tx}-\text{RIS}}$ is the distance between the transmitter and the center of the RIS, $\boldsymbol{\delta}^{\text{Tx}-\text{RIS}} = \left(\sin\theta^{\text{Tx}-\text{RIS}}\cos\phi^{\text{Tx}-\text{RIS}}, \sin\theta^{\text{Tx}-\text{RIS}}\sin\phi^{\text{Tx}-\text{RIS}}\right)^T$ is the u-v representation of the direction from Tx toward RIS.

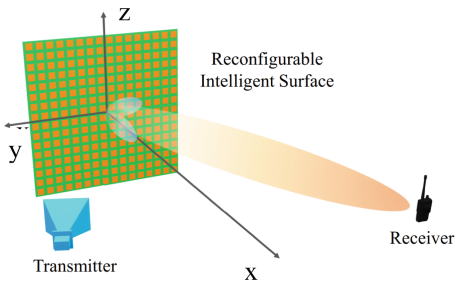

Fig. 1. RIS-aided wireless communication system model [6].

The channel gain between the unit cell (m, n) of the RIS and the transmitter can be given as [6]:

$$h_{m,n}^{\text{Tx - RIS}} = \frac{\lambda\sqrt{G_{m,n}^{\text{Tx - RIS}} G_{m,n}^{\text{RIS - Rx}}}}{4\pi d_{m,n}^{\text{Tx - RIS}}} \exp\left(-j\frac{2\pi}{\lambda} d_{m,n}^{\text{Tx - RIS}}\right), \tag{2}$$

where λ is the wavelength of the EM wave. $G_{m,n}^{\text{RIS - Tx}}$ and $G_{m,n}^{\text{RIS - Rx}}$ are the gains of a unit cell (m, n) of the RIS towards the transmitter and receiver, respectively. $d_{m,n}^{\text{Tx - RIS}}$ is the distance between the transmitter and the unit cell (m, n) in the RIS. In the same way, we can derive the channel gain between the unit cell (m, n) of the RIS and the receiver as:

$$h_{m,n}^{\text{RIS - Rx}} = \frac{\lambda\sqrt{G_{m,n}^{\text{RIS - Rx}} G_{m,n}^{\text{Rx - RIS}}}}{4\pi d_{m,n}^{\text{RIS - Rx}}} \exp\left(-j\frac{2\pi}{\lambda} d_{m,n}^{\text{RIS - Rx}}\right), \tag{3}$$

The unit cell of the RIS is designed with a special design structure. It is equipped with a control element (e.g., a PIN diode) to manipulate the amplitude and phase of the impinging EM wave. The unit cell receives the EM wave from the transmitter and adjusts its amplitude and phase with the control element. Then, the manipulated EM wave is reflected and re-radiated to the air [6]. The total received signal at the receiver can be given as:

$$y = \left(\sum_{m=0}^{M-1}\sum_{n=0}^{N-1} h_{m,n}^{\text{Tx - RIS}} h_{m,n}^{\text{RIS - Rx}} \Gamma_{m,n} + h^{\text{Tx - Rx}}\right) x^{\text{Tx}}, \tag{4}$$

where $\Gamma_{m,n}$ is reflection coefficient of the unit cell (m, n). $h^{\text{Tx - Rx}}$ is the direct channel between the transmitter and the receiver. x^{Tx} is the transmitted wave from the transmitter. The additive white Gaussian noise caused by the thermal noise of the receiver circuit is ignored in (4) since the noise level is negligible compared to the received signal in the wireless communication system.

3 RIS Channel and DOT Estimation

3.1 Channel Estimation

To enable adaptive beamforming, the channel state information needs to be acquired by channel estimation method. Several existing channel estimation methods have been developed for the RIS-aided system [3–6]. In this paper, we present a fundamental efficient channel estimation algorithm based on the least square method. We first introduce an orthogonal training matrix as the training pilots of the RIS system. Any orthogonal matrix can be used to train the RIS, however, we use Hadamard matrix in this work. We can build the Hadamard matrix with the size of 2^k by using the following equation.

$$\mathbf{Q}_2 = \begin{bmatrix} 1 & amp; 1 \\ 1 & amp; -1 \end{bmatrix}, \quad \mathbf{Q}_{2^k} = \begin{bmatrix} \mathbf{Q}_{2^{k-1}} & amp; \mathbf{Q}_{2^{k-1}} \\ \mathbf{Q}_{2^{k-1}} & amp; -\mathbf{Q}_{2^{k-1}} \end{bmatrix}. \tag{5}$$

Hence, with the number of unit cells of the RIS (i.e., MN) being the power of 2, the training matrix $\mathbf{G}$ is $\mathbf{Q}_{MN}$**.** To realize the direct channel between Tx and Rx (i.e., $h^{\mathrm{Tx-Rx}}$), we add one more training vector with all -1 value to the training matrix such that.

$$\mathbf{G} = [\mathbf{Q}_{MN}; -1], \tag{6}$$

where $1 \in \boldsymbol{Z}^{MN}$ is unit vector of all 1.

To this end, we rewrite the total receive signal in (4) in matrix form as follows.

$$\bar{y} = \boldsymbol{\Gamma}^T \mathbf{h} + \mathrm{h}^{\mathrm{Tx-Rx}}, \tag{7}$$

where $\bar{y} = \frac{y}{x^{\mathrm{Tx}}}$, $\mathbf{h}$ and $\boldsymbol{\Gamma}$ are, respectively, the channel gain vector and reflection coefficient vector with size of MN, obtained by vectorization of $h_{m,n}^{\mathrm{Tx-RIS}} h_{m,n}^{\mathrm{RIS-Rx}}$ and $\Gamma_{m,n}$. After training the RIS with the training matrix $\mathbf{G}$, we obtain the received signal vector (i.e., $\bar{\boldsymbol{y}}$) as

$$\begin{aligned} \bar{\boldsymbol{y}} &= \mathbf{G}\mathbf{h} + \mathrm{h}^{\mathrm{Tx-Rx}} \\ &= \mathbf{G}\bar{\mathbf{h}}, \end{aligned} \tag{8}$$

where $\bar{\mathbf{h}} = \left[\mathbf{h}; \mathrm{h}^{\mathrm{Tx-Rx}}\right]$. The problem in (8) becomes a linear problem, and a solution can be acquired by the least square estimator such as

$$\hat{\mathbf{h}} = \frac{\bar{\mathbf{G}}^{\mathbf{T}} \bar{\mathbf{y}}}{\bar{\mathbf{G}}^{\mathbf{T}} \bar{\mathbf{G}}}. \tag{9}$$

The solution in (9) is the estimated channel or the channel state information (CSI) of the RIS-aided system.

3.2 RIS-Based DoT Estimation

Direction of transmission (DoT) is the direction of reflected beam from the RIS toward the desired receiver. Note that the channel information includes the direction of the transmitter toward RIS (i.e., $\boldsymbol{\delta}^{\mathrm{Tx-RIS}}$) and the direction of the RIS toward the receiver (i.e., $\boldsymbol{\delta}^{\mathrm{RIS-Rx}}$). Under the far-field assumption, the channel gains between RIS and the receiver are sparse in the angular domain. To reveal the sparsity of the channel gains, we use the two-dimension discrete Fourier transform (2D-DFT) to transform the channel gains into the angular domain. The 2D-DFT of $\hat{h}_{m,n}$ for $m = 1, \ldots, M$ and $n = 1, \ldots, N$ can be derived as:

$$\mathcal{F}\left(\hat{h}_{m,n}\right)_{k,l} = \frac{1}{MN} \sum_{m=1}^{M} \sum_{n-1}^{N} \hat{h}_{m,n} \exp\left(-j2\pi\left(\frac{k}{M}m + \frac{l}{N}n\right)\right), \tag{10}$$

for $k = 1, \ldots, M$ and $l = 1, \ldots, N$.

The point that matches to the DoT results in the maximum value of the 2D-DFT. Thus, we can realize the maximum point such as

$$k^*, l^* = \underset{\substack{\mathrm{k} = 1, \ldots, \mathrm{M} \\ l = 1, \ldots, N}}{\operatorname{argmax}} \mathcal{F}\left(\hat{h}_{m,n}\right)_{k,l}. \tag{11}$$

Then, the tuple $\left(\frac{k^*}{M}, \frac{l^*}{N}\right)$ corresponds to the u-v representation of the DoT. By simple mathematical transformation, one can obtain the azimuth and elevation angles of the DoT.

4 Proposed Approach

Due to the imperfection of the manufacturing and experimental setting, the beam may not exactly be directed in the desired direction, which reduces the power received at the receiver. Moreover, in practical scenarios, the RIS should perform adaptive beam tracking according to the position of the mobile receiving devices. Besides, RIS beams may interfere with other transmitters/receivers, or they may be interfered with by others. In order to tackle this, we propose a four-step scheme allowing us to localize the receiver, focus the power on the receiver direction, and suppress interferences. The procedure of this scheme is presented in Fig. 2. These steps are presented in the next sections.

Each step is explained as follows:

- **Estimate the channel**: The channel will be estimated by training the RIS. Note that the total received signal is changed according to the reflection coefficient vector as mentioned in (4). By sending the signal with L (e.g., 256 in this paper) independent patterns based on the Hadamard matrix as training pilots, L channels between each unit cell of the RIS are estimated by multiplying the received signals with the inversion of L transmitting patterns. The final optimal channel can be obtained by applying the least square estimator [6].
- **Determine the direction of the receiver**: Based on the estimated channel, the direction of the receiver can be derived.

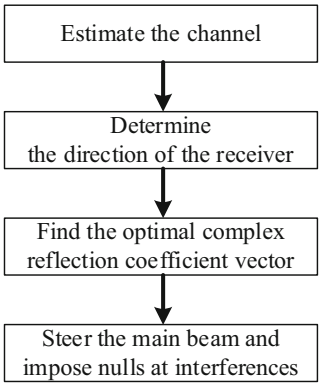

Fig. 2. The four-step proposed scheme.

- **Find the optimal complex reflection coefficient vector:** To form the main beam towards the receiver with the constraint of imposing nulls at the direction of interferences, the least squares method is adopted to calculate the optimal complex reflection coefficient vector. This step is described in detail below.
- **Steer the main beam and impose nulls at interferences:** After obtaining the optimal complex reflection coefficient vectors, these vectors can be applied to the RIS. Therefore, the main beam can be focused on the receiver direction and interferences can be suppressed by imposing nulls at the direction of the jammers.

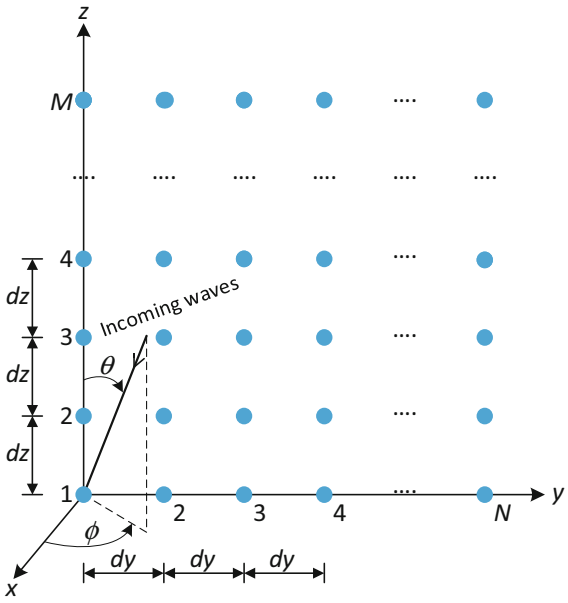

Fig. 3. A RIS with $M \times N$ unit cells.

Considering a RIS with $M \times N$ unit cells as shown in Fig. 3. The scattering field from the RIS can be theoretically expressed as [7, 8]:

$$E(\phi, \theta) = \sum_{m=0}^{M-1} \sum_{n=0}^{N-1} w_{m,n} \Gamma_{m,n} f_{m,n}(\phi, \theta) e^{j(m\psi_z + n\psi_y)}, \tag{12}$$

where:

- $w_{m,n} = A_{m,n} e^{j\alpha_{m,n}}$ is the complex weights, where $A_{m,n}$ and $\alpha_{m,n}$ are the amplitude and the phase of the (m, n) unit cell, respectively. For simplicity, in this paper, the amplitude and the phase of all unit cells are 1 and 0, respectively;
- $\Gamma_{m,n} = a_{m,n} e^{j\delta_{m,n}}$ is the complex reflection coefficient, where $a_{m,n}$ and $\delta_{m,n}$ are the reflection amplitude and the phase of the (m, n) unit cell, respectively;
- $f_{m,n}(\phi, \theta)$ is the element factor of the unit cell at (ϕ, θ);
- $\psi_z = \kappa d_z \cos(\theta)$; $\psi_y = \kappa d_y \sin(\theta) \sin(\phi)$; $\kappa = 2\pi/\lambda$; $d_z = d_y = \lambda/2$.

The scattering EM wave from the RIS can be controlled and formed by adjusting the reflection amplitude $\left(a_{m,n}\right)$ and phase $\left(\delta_{m,n}\right)$ of each unit cell. Therefore, the scattering field can be expressed in the matrix form [9]:

$$E(\phi, \theta) = \mathbf{f}(\phi, \theta)\mathbf{s}(\phi, \theta)\mathbf{\Gamma} \tag{13}$$

where:

- $\mathbf{s}(\phi, \theta) = \left[s(\phi, \theta)_1, \ldots, s(\phi, \theta)_{MN}\right]$: the steering vector of the RIS;
- $\mathbf{\Gamma} = [\Gamma_1, \ldots, \Gamma_{MN}]^T$: the complex reflection coefficient vector;
- $\mathbf{f}(\phi, \theta)$: the vector of element factor which is assumed to be 1 in this paper.

Assuming that the optimal complex reflection coefficient vector is as follows:

$$\mathbf{\Gamma_o} = \mathbf{\Gamma_{ref}} - \mathbf{x}, \tag{14}$$

where:

- $\mathbf{\Gamma_{ref}}$: the reference reflection coefficient vector which can be obtained by using the Chebyshev method;
- $\mathbf{\Gamma_o}$: the optimal reflection coefficient vector;
- $\mathbf{x}$: the perturbation of the reflection coefficient vector.

The optimal scattering field can be rewritten as:

$$E_o(\phi, \theta) = \mathbf{s}(\phi, \theta)\mathbf{\Gamma} = \mathbf{s}(\phi, \theta)(\mathbf{\Gamma_{ref}} - \mathbf{x},), \tag{15}$$

$$\Leftrightarrow E_o(\phi, \theta) = \mathbf{s}(\phi, \theta)\mathbf{\Gamma_{ref}} - \mathbf{s}(\phi, \theta)\mathbf{x}. \tag{16}$$

To impose K nulls in the directions of $(\phi, \theta)_k = \left[(\phi, \theta)_1, \ldots, (\phi, \theta)_K\right]$ with $k = 1, \ldots, K$, $E_o(\phi, \theta)$ is set equal to zero, and the resultant equations are then written as:

$$\mathbf{s}(\phi, \theta)\mathbf{x} = \mathbf{s}(\phi, \theta)\mathbf{\Gamma_{ref}}, \tag{17}$$

$$\Leftrightarrow \mathbf{Sx} = \mathbf{E_{ref}}, \tag{18}$$

where:

$$\mathbf{S} = \begin{bmatrix} s(\phi_1,\theta_1)_1 & s(\phi_1,\theta_1)_2 & \cdots & s(\phi_1,\theta_1)_{MN} \\ s(\phi_2,\theta_2)_1 & s(\phi_2,\theta_2)_2 & \cdots & s(\phi_2,\theta_2)_{MN} \\ \vdots & \vdots & \ddots & \vdots \\ s(\phi_K,\theta_K)_1 & s(\phi_K,\theta_K)_2 & \cdots & s(\phi_K,\theta_K)_{MN} \end{bmatrix}, \tag{19}$$

$$\mathbf{x} = [x_1, \ldots, x_{MN}]^T, \tag{20}$$

$$\mathbf{E_{ref}} = [\mathbf{s}(\phi_1,\theta_1)\mathbf{\Gamma_{ref}}, \ldots, \mathbf{s}(\phi_K,\theta_K)\mathbf{\Gamma_{ref}}]^T \tag{21}$$

Equation (18) can be solved by applying the method of least squares (LS):

$$\mathbf{x} = \mathbf{S}^{\dagger}\left(\mathbf{S}\mathbf{S}^{\dagger}\right)^{-1}\mathbf{E_{ref}}. \tag{22}$$

Substituting (22) into (14), the optimal complex reflection coefficient vector is obtained, and the optimal pattern is formed.

5 Numerical Results

The performance of the proposed approach is evaluated through several scenarios by simulation in this section.

5.1 Parameter Setup

All scenario simulations use the following parameters if not specifically specified:

- A horn antenna works as an EM source. The RIS includes 16 × 16 unit cells. The receiver is equipped with a single antenna. The direction of interferences and jammers is assumed to be known in advance;
- The target operating frequency is chosen as 5.8 GHz in the industrial, scientific, and medical band;
- The reference coefficient vector is obtained by using the Chebyshev method with the side lobe level (SLL) of −20 dB;
- The illustrative results for all scenarios are taken as an average of over 50 simulations in MATLAB 2023a with an Intel® Xeon® Intel® Gold 5115 processor;
- Besides demonstrating the ability of the proposed approach, this approach is also compared to the interference suppression solution based on the bat algorithm which is mentioned as the nature-inspired optimization (NIO) method in this paper. In the same manner in the paper [10, 11], the fitness function is built as (23). Some important parameters are set as in [10, 11]: the penalty parameter ξ is 1000; the population is 500; the number of iterations is 100.

$$F(\mathbf{\Gamma}, \phi_k, \theta_k, \xi) = \sum_{\phi \neq \phi_k,\, \phi=-90^\circ}^{\phi=90^\circ} \left[\left| E_o(\phi,\theta_k) - E_{ref}(\phi,\theta_k) \right|^2 \right] + \xi \sum_{k=1}^{K} \left[\left| E(\phi_k,\theta_k) \right|^2 \right] \tag{23}$$

where: $E_{ref}(\phi, \theta_k)$, $E_o(\phi, \theta_k)$, and $E(\phi_k, \theta_k)$ are the reference field, the optimal field at (ϕ, θ_k), and the optimal field at (ϕ_k, θ_k), respectively.

5.2 Wireless Communication with the Capacity to Suppress Interferences

This subsection presents the ability to focus the main beam towards the receivers and to impose null at the direction of interferences. After estimating the channels between the transmitter and the RIS and between the RIS and the receiver based on the least square estimator, the direction of the receiver can be attained based on the estimated channels. From that, RIS is capable of steering the beam to the receiver direction. Figure 4 shows the 2D pattern of the RIS with the main beam towards the receiver at $(\phi, \theta) = (0°, 90°)$ and with a null imposed at the direction of the interference $(\phi_k, \theta_k) = (25°, 90°)$. It is clear that the main beam of the LS-based pattern is precisely steered towards the receiver and the proposed approach sets a strong null at an interference with -326.78 dB which is more than 250 dB deeper than the null for the NIO-based pattern. Besides, the proposed approach-based pattern can well maintain the SLL as the reference pattern. Figure 5 displays the amplitude and phase distribution matrix of reflection coefficients for the RIS for the scenario in Fig. 4.

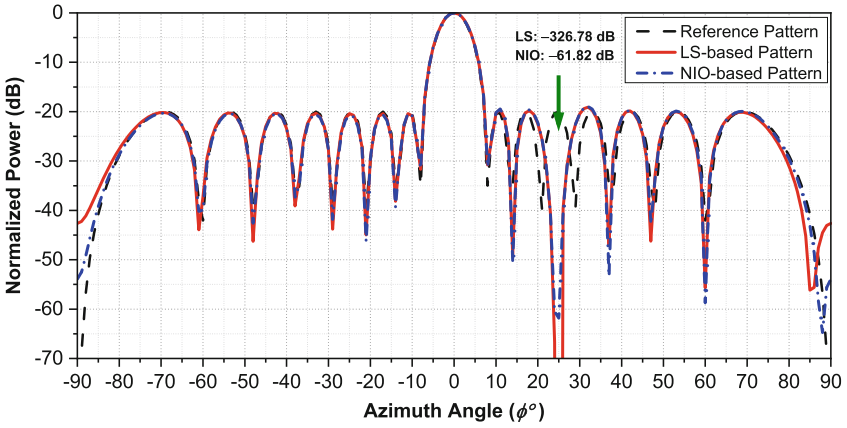

Fig. 4. The 2D pattern of the RIS with the main beam at $(\phi, \theta) = (0°, 90°)$ and an interference at $(\phi_k, \theta_k) = (25°, 90°)$.

However, in reality, the interferences may be present in a wide range or an interference that appears continuously overtime over an angular range. To solve this problem, interference suppression in a wide range is really essential. The next scenario assumes interferences in the range from $-45°$ to $-35°$. Figure 6 indicates that the proposed approach suppresses radiation at $(\phi_k, \theta_k) = [-45° : -35°, 90°]$ while it still maintains the main beam towards the receiver. The null depth levels of the LS-based pattern are almost deeper than -65 dB, and the proposed approach outperforms the NIO-based approach in terms of not only sidelobe control but also interference suppression ability. When the receiver changes position, the receiver's direction relative to the RIS also changes.

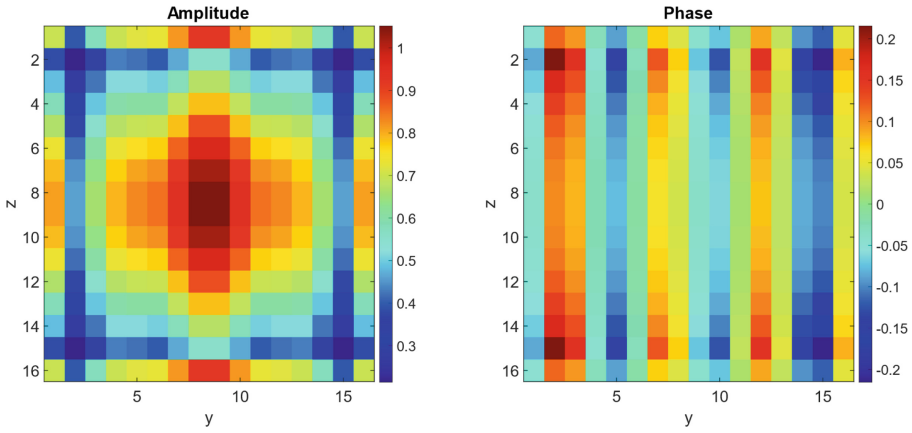

Fig. 5. Amplitude and phase distribution matrix of reflection coefficients for the RIS.

Therefore, the proposed approach needs to be to steer the beam flexibly in space towards the desired direction. To demonstrate this ability, Figs. 7 and 8 show the 2D and 3D pattern of the RIS in the case of the receiver at $(\phi, \theta) = (10°, 80°)$ and interferences at $(\phi_k, \theta_k) = ([40° : 50°], 80°)$, respectively. The LS-based pattern still shows that it is able to steer the main beam toward the receiver while suppressing interferences and it outperforms the NIO-based pattern in every aspect. Similar to this beam steering scenario, Fig. 9 shows the results of steering the main beam towards $(\phi, \theta) = (40°, 60°)$ and suppressing the interference that appears at $(\phi_k, \theta_k) = ([0° : 10°], 60°)$. The results demonstrate that the proposed approach is really effective when the main beam is not only steered toward the $(\phi, \theta) = (0°, 90°)$ direction but also toward many other directions.

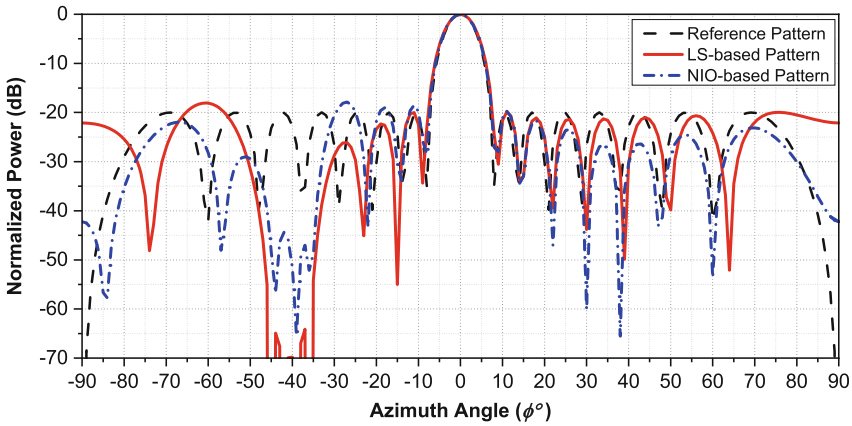

Fig. 6. The 2D pattern of the RIS with the main beam at $(\phi, \theta) = \left(0°, 90°\right)$ and interferences at $(\phi_k, \theta_k) = \left[-45° : -35°, 90°\right]$.

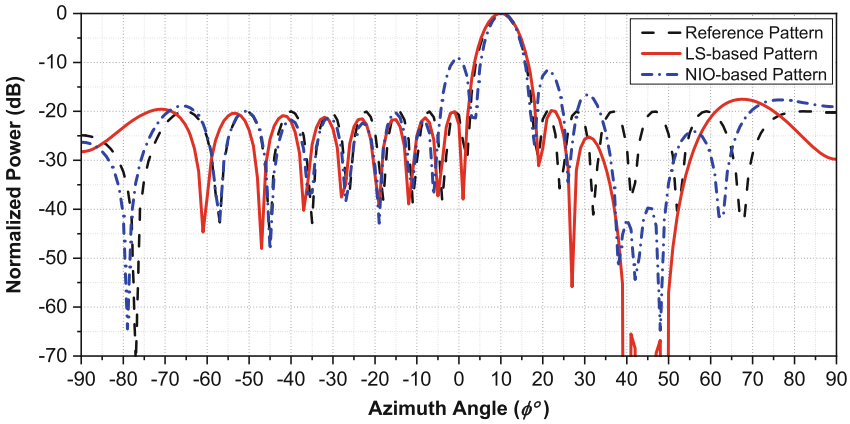

Fig. 7. The 2D pattern of the RIS with the main beam at $(\phi, \theta) = \left(10°, 80°\right)$ and interferences at $(\phi_k, \theta_k) = \left(\left[40° : 50°\right], 80°\right)$.

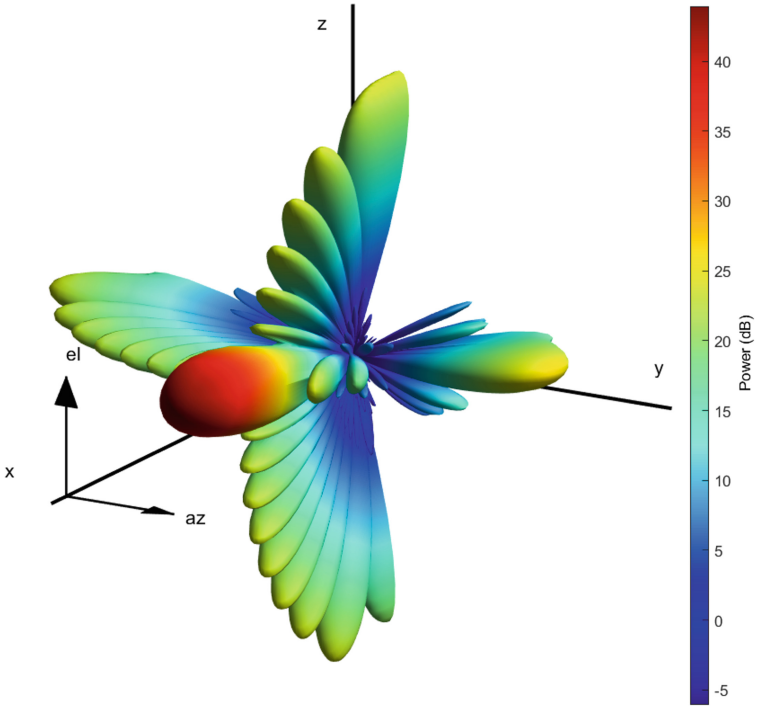

Fig. 8. The 3D pattern of the RIS with the main beam at $(\phi, \theta) = \left(10°, 80°\right)$ and interferences at $(\phi_k, \theta_k) = \left(\left[40° : 50°\right], 80°\right)$.

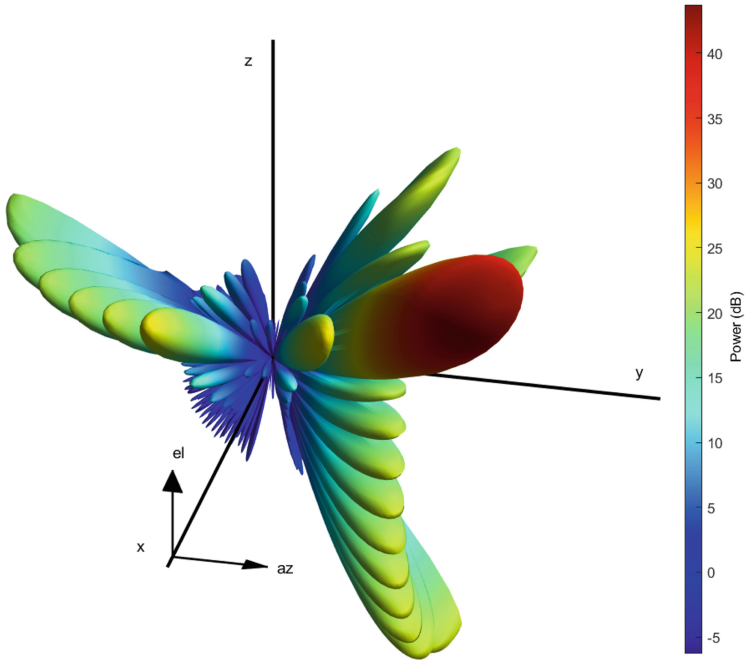

Fig. 9. The 3D pattern of the RIS with the main beam at $(\phi, \theta) = \left(40°, 60°\right)$ and interferences at $(\phi_k, \theta_k) = \left(\left[0° : 10°\right], 60°\right)$.

6 Conclusion

In this paper, an approach based on the method of least squares for RIS-aided wireless communication is proposed. This study makes a contribution to the ever-growing body of knowledge in RF wireless communication and RIS. It offers a robust and practical solution tailored to the demands of the emerging IoT landscape, where efficient and interference-free wireless communication is paramount. Specifically, the four-step proposed approach, which includes: (i) estimate the channel; (ii) determine the direction of the receiver; (iii) find the optimal complex reflection coefficient vector; (iv) and steer the main beam and impose nulls at interferences, is applied and verified via some scenarios. The proposed approach with the ability to steer the main beam towards the receiver and suppress interferences has shown outperformance relative to the NIO-based approach with respect to both sidelobe control and interference suppression ability. In future works, a system with multiple antennas in the transmitter and the receiver; or applying RIS-aided wireless communication to integrated sensing and communication in 6G wireless communication systems should be considered.

Acknowledgment. This research is supported by Hanoi University of Industry [Grant number: 29–2023-RD/HĐ-ĐHCN].

References

1. Xie, L., Shi, Y., Hou, Y.T., Lou, A.: Wireless power transfer and applications to sensor networks. IEEE Wireless Commun. **20**(4), 140–145 (2013)
2. Kamalinejad, P., Mahapatra, C., Sheng, Z., Mirabbasi, S., Leung, V.C., Guan, Y.L.: Wireless energy harvesting for the internet of things. IEEE Commun. Mag. **53**(6), 102–108 (2015)
3. Choi, K.W., et al.: Simultaneous wireless information and power transfer (SWIPT) for internet of things: novel receiver design and experimental validation. IEEE Internet Things J. **7**(4), 2996–3012 (2020)
4. Cui, T.J., Qi, M.Q., Zhao, J., Cheng, Q.: Coding metamaterials, digital metamaterials and programmable metamaterials. Light Sci. Appl. **3**(e218) (2014)
5. Li, Y.B., et al.: Transmission-type 2-bit programmable metasurface for single-sensor and singlefrequency microwave imaging. Sci. Rep. **6**(23731) (2016)
6. Nguyen, M.T.: Reconfigurable intelligent surface beam focusing for performance enhancement of wireless power transfer systems: a theoretical and experimental study. Ph.D. dissertation, Department of Electrical and Computer Engineering, Sungkyunkwan University, South Korea (2022)
7. Yang, H., et al.: A programmable metasurface with dynamic polarization, scattering and focusing control. Sci. Rep. **6**(1) (2016)
8. Kha, H.M., et al.: An efficient beamformer for interference suppression using rectangular antenna arrays. J. Commun. **18**(2), 116–122 (2023)
9. Kha, H.M., et al.: A null synthesis technique-based beamformer for uniform rectangular arrays. In: 2022 International Conference on Advanced Technologies for Communications (ATC), pp. 13-17 (2022)
10. Tong, L., Nguyen, C., Le, D.: An effective beamformer for interference mitigation. In: Anh, N.L., Koh, SJ., Nguyen, T.D.L., Lloret, J., Nguyen, T.T. (eds.) Intelligent Systems and Networks. Lecture Notes in Networks and Systems, vol. 471, pp. 630–639. Springer, Singapore (2022). https://doi.org/10.1007/978-981-19-3394-3_73
11. Luyen, T.V., et al.: An efficient ULA pattern nulling approach in the presence of unknown interference. J. Electromagn. Waves Appl. **35**(1), 1–18 (2020)